Journal of Applied Electrochemistry (2005) 35:449–458
DOI 10.1007/s10800-004-8345-3

The Influence of electrochemical surface modifications on naval steel corrosion

C. F. ZINOLA[1,*], V. DÍAZ[2], S. MARTÍNEZ[2] and J. RODRÍGUEZ[1]
[1]*Electrochemistry Laboratory, School of Sciences, Libertad Street No. 2497, 11400, Montevideo, Uruguay*
[2]*Engineering School, Universidad de la República, Julio Herrera y Reissig 565, 11300, Montevideo, Uruguay*
*(*author for correspondence, e-mail: fzinola@fcien.edu.uy)*

Received 08 June 2004; accepted in revised form 12 December 2004

Key words: corrosion, electrochemical methods, naval steel, surface modifications, voltammograms

Abstract

The corrosion behaviour of naval steels is characterized by cyclic voltammetric profiles, open-circuit potential decays and polarization curves in 0.5 M sodium nitrate and in 0.6 M sodium chloride at 20 °C. Naval steel surfaces can be modified by the application of periodic symmetric and/or asymmetric potential routines in strong alkaline solutions. These perturbations produce the formation of protective or non-protective surface oxides, which can be characterized by scanning electron microscopy and cyclic voltammetry. Corrosion parameters of the new surface oxides are evaluated by polarization curves after long-time exposures in electrolytes containing sodium chloride and sodium nitrate.

1. Introduction

Steel corrosion in marine atmospheres or underwater environments has been studied for many decades due to its technological applications [1, 2]. Among the wide spectra of applications that steel is able to cover, those from shipping-manufacture and buildings are the most attractive of all. In the case of ships, the hull structure, which acts as the massive load support for upper decks, is one of the most susceptible zones to corrosion where the steel surface can be degraded to a critical thickness. The performance of conventional corrosion protection methodologies, such as cathodic protection, organic coatings or inhibitors is not effective for the expected design lifetimes [3, 4]. Therefore, it was decided to study new methodologies based on periodic potentials with the aim of preparing certain types of oxide, on naval steel with different corrosion behaviours.

Steel corrosion in seawater is a well-known metal degradation mechanism [5, 6]. The formation of the earlier stages of iron oxides strongly depends on the chemical composition of steel and seawater [7]. However, this complex process can be modified by surface pretreatments that can change the nature of the oxygen-containing precursor of the bulk oxides. In this paper, we propose a new electrochemical methodology for changing the original surface oxide morphology of steel by using periodic potential perturbations (PPP). Previous studies on noble electrodes in acid media have demonstrated the possibility of changing the distribution of the surface crystallography and surface roughness using these methodologies [8]. The application of these PPP on metal electrodes produces either temporary or permanent morphological changes, depending on the applied frequency and potential limits [9–11]. Thus, the application of a fast (larger than 2 kHz) symmetric PPP on noble metal electrodes in acid media develops new crystallographic planes without changes in the surface roughness [11, 12]. The electrochemical responses and scanning tunnelling microscopic images of the resulting electrodes are generally different from the original surfaces, depicting stepped crystalline planes with low Miller indices [8]. The electrocatalytic properties of the modified substrates exhibit new interesting features with industrial applications in electrosynthesis and fuel cell technology [12–14]. On the other hand, some works have reported the application of sinusoidal potential perturbations on ferrous metals, chromium and copper alloys in chloride-containing solutions, where material degradation and corrosion products have been analysed [15–17]. An alternating current process was performed on 304 stainless steel and the passive properties of the resulting oxides were determined by recording the critical current density and the passive current density with time for open-circuit potential decay in 0.1 M H_2SO_4 [18]. In this work it is proposed that the application of a PPP technique to naval steels with a symmetric/asymmetric signal in a strong alkaline solution, i.e. a more suitable electrolyte for the growth of surface oxides with good stability to enhance corrosion resistance after long time exposures in acid electrolytes [19].

2. Experimental details

2.1. *General*

Electrochemical experiments were carried out at 20 °C in a conventional three electrode cell using naval steel rods (ca. 0.5 cm^2 geometric area) as working electrodes. Table 1 shows the chemical composition of the working electrode. The electrochemical set-up was completed using a large-area-platinum counter electrode and a saturated calomel reference electrode (*sce*) in another compartment to avoid further chloride diffusion into the main cell. All potentials in the text are referred to the *sce* scale.

2.2. *Surface characterization*

The electrochemical surface characterization of naval steels was performed by cyclic voltammetry between −1.5 and 1.5 V run at 0.008 V s^{-1} in aqueous 0.50 M sodium nitrate (analytical J. T. Baker) with a Radiometer Copenhagen PGP 201 Potentiostat–Galvanostat. The current vs. potential profiles was recorded on a GOERZ Paper Recorded, Servogor No. 790 Model or digitally *via* a personal computer. In the latter case, integrated charge vs. potential curves were used to calculate the charge densities under the characteristic peaks after a graphical deconvolution. For the application of the PPP methodology in 2 or 5 M sodium hydroxide (analytical Biopack), the same Potentiostat was employed coupled with a LYP WT Model Square Wave Function Generator. Data acquisition and corrosion analysis was performed with Voltamaster 1 Software of Radiometer (Copenhagen) and checked as explained above. All solutions are prepared from MilliQ–Milliplus water (resistivity > 18.2 MΩ cm).

2.3. *Surface pre-treatments*

The initial surface morphology of naval steels was also studied using different pre-treatments. Before each pre-treatment, the steel surface was mechanically polished with emery paper up to a 600 grid and subsequently rinsed in MilliQ-Milliplus water. For the polished surfaces the following treatments were applied:

(i) Chemical etching in a hot 1:1 concentrated sulphuric acid: nitric acid mixture for 25 min.
(ii) Thermal pre-treatment of the steel rod in a propane:butane/oxygen flame during 30 min till a red-coloured texture.
(iii) Triangular potential programs run at 2.5 V s^{-1} between −2.5 and 2.5 V in 2 and 5 M sodium hydroxide to activate the surface for 300 cycles.

2.4. *Potential perturbation*

For the chemically etched naval steel surface, a PPP technique in either 2 or 5 M sodium hydroxide was applied in three different manners;

(a) Symmetric square wave at a given frequency (f) between an upper and a lower potential value (E_u and E_l, respectively).
(b) Asymmetric square wave between an upper and a lower potential (E_u and E_l with an upper hemiperiod (f_u) at E_u different from the lower hemiperiod value (f_l) at E_l.
(c) Subsequent (symmetric and asymmetric) square wave at distinct f(f_l and f_u) between different E_u and E_l values.

2.5. *Morphological studies*

A Jeol JSM-5900 LV Scanning Electron Microscope checked the morphology of the resulting naval steel surfaces. The filament used in this work was hairpin tungsten and the input voltage for all the images was 15 kV using a secondary electron detector.

2.6. *The influence of chloride for long-time exposures*

The influence of chloride on naval steel corrosion was studied in different concentrations (0.01, 0.10 and 0.60 M) of sodium chloride (Mallinckrodt analytical) in the presence and in the absence of 0.50 M sodium nitrate (working solutions) after 1 h, 24 h, 48 h and 1 week. To study corrosion parameters in aerated solutions, potentiostatic polarization curves were run from the rest potential of the interface to ±20 mV, from which the corrosion potential (E_{corr}) and the corrosion current density (j_{corr}) were calculated using the Voltamaster software. The obtained values were checked with the method proposed by Rocchini [20] showing good accordance within ±1 mV.

2.7. *Oxide stability*

The stability of surface oxides grown by symmetric, asymmetric and combined PPP was checked in 0.10 M sulphuric acid (analytical J. T. Baker), 0.50 sodium nitrate, 0.60 M sodium chloride and a mixed solution of 0.50 sodium nitrate and 0.60 M sodium chloride. The

Table 1. Naval steel chemical mean composition (%) derived from atomic absorption spectrophotometric measurements

Chemical Composition	C	Mn	Si	S	P	Cu	Sn	Cr	Ni	Mo	V	Nb	W
Mean in weight 1%	0.085	1.529	0.244	0.025	0.016	0.090	0.003	0.027	0.035	0.013	0.004	0. 003	0.002

open-circuit potential was followed as a function of time immediately after the application of the signal. The same equipment and solutions were employed as explained above.

3. Results and discussion

3.1. *Electrochemical behaviour of naval steels in aqueous 0.50 M sodium nitrate*

Anions have been considered as aggressive or inhibitive with respect to metal passivity breakdown [21]. Therefore, halide anions promote the local destruction of a passive layer initiating pitting corrosion, whereas other anions, such as, nitrate, chromate and phosphate can exercise an inhibition effect that prevents pitting corrosion. In the case of sulphate anions different results have been found, but it generally stimulates homogeneous metal dissolution [21, 22].

The corrosion behaviour of naval steel has been previously studied in our lab in perchlorate, nitrate and sulphate aqueous solutions to evaluate the inhibiting or aggressive contributions to the surface. In sodium perchlorate supporting electrolyte, large dissolution currents for naval steel can be detected together with perchlorate reductive decomposition to chloride. On the other hand, the passive film is thickened in sulphate solutions during long-time experiments. This fact has also been reported in sulphate and silicate solutions [23] with the determination of Fe(II) and Fe(III) soluble species using rotating ring (gold) – disc (iron) techniques. The effects of inorganic anions on the corrosion behaviour and pitting of steel have been also studied in the presence of chloride [24]. It has been found that the inhibitive effect decreases from phosphate, chromate, nitrate to sulphate anions. Therefore, to minimize problems between anion inhibition and passive thickening, nitrate has been selected as the working anion for comparison purposes.

Figure 1 shows the repetitive voltammetric response of a polished naval steel electrode in 0.50 M sodium nitrate run at 0.008 V s^{-1} between −1.50 and 1.50 V. The positive going potential scan exhibits a complex contour with one hump at −0.75 V and an anodic broad peak, denoting the formation of two bulk iron oxides [7], at 0.15 V with a charge density of 180 μC cm^{-2}, denoting almost a full monolayer metal oxidation. The passivation of the steel surface takes place from 0.8 to 1.1 V in 0.50 M sodium nitrate. In the reverse negative scan, a reactivation process is observed through a medium-intensity peak located at −0.38 V which shows a fast oxidation after the reduction of iron oxides (50 μC cm^{-2} in one cycle). At −0.60 V an inflection current is observed with another hump before the hydrogen evolution reaction is observed at −1.15 V.

Potentiostatic polarization curves were run in a fully aerated 0.50 M sodium nitrate solution from which $E_{corr} = -0.627$ V and $j_{corr} = 2$ μA cm^{-2} were calculated.

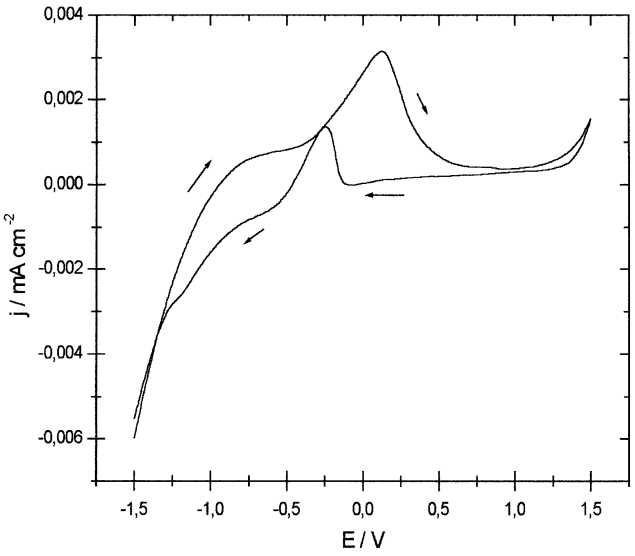

Fig. 1. Repetitive cyclic voltammogram of polished naval steel run between −1.50 and 1.50 V at 0.008 V^{-1} in 0.50 M aqueous sodium nitrate containing dissolved oxygen. Temperature = 20 °C. The arrows indicate the potential cycling direction.

3.2. *Comparison between different electrode pre-treatments*

Several electrode pre-treatments were compared to determine the best initial condition previous to the application of the PPP techniques. In all cases, each naval steel surface was polished with emery paper to eliminate all the surface oxides. Figure 2 (a–c) shows the cyclic voltammetric runs between −1.50 and 1.50 V run at 0.008 V s^{-1} for the three pre-treatments in a fully aerated 0.50 M sodium nitrate solution.

3.2.1. *Chemical etching*

Figure 2(a) shows the repetitive cyclic voltammogram of the steel surface after 5 min of chemical etching in a hot sulphuric/nitric bath. The current vs. potential profile is totally different from that for the polished naval steel. Two main features of the new response are a low-intensity reactivation peak (at ca. −0.6 V) and an increased bulk oxidation peak leading to passivation at 0.85 V with 260 μC cm^{-2} of charge density, which is more than one monolayer. These results show that chemical etching produces more stable surfaces because of the negligible reactivation during cathodic scans.

The calculated corrosion parameters from potentiostatic polarization curves in aerated 0.50 M sodium nitrate are $E_{corr} = -0.601$ V, $j_{corr} = 40\mu$A cm^{-2}. *SEM* micrographs of these surfaces exhibited a smooth surface morphology in comparison to the untreated sample, with randomly distributed fissures, as well as surface oxide residues (Figure 3). These fissures explain the larger current density value observed for j_{corr} (edges and kinks of the fissure borders).

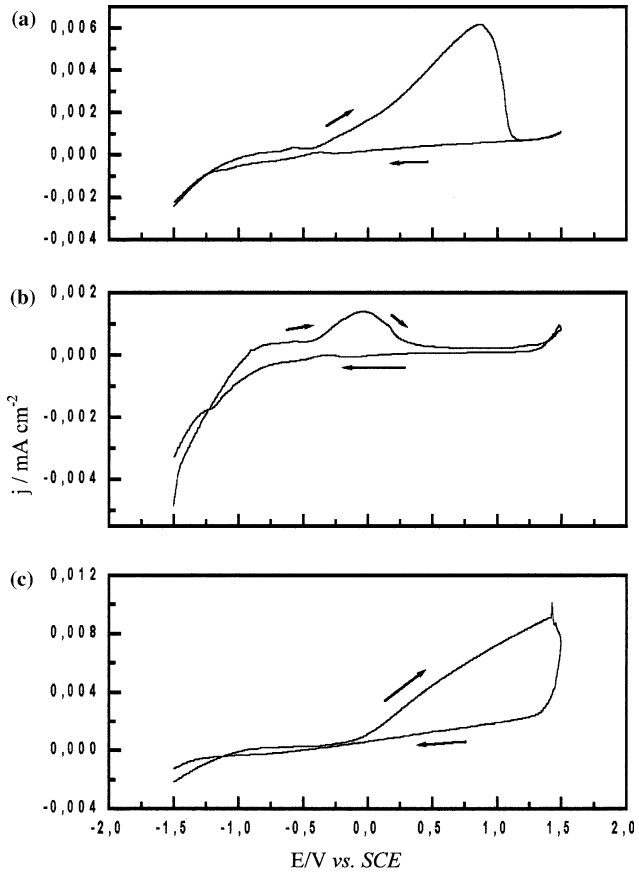

Fig. 2. (a) Stable cyclic voltammogram of chemical treated (sulphuric/nitric) naval steel for 5 min; (b) Stable cyclic voltammogram of thermally treated naval steel for 30 min; (c) Stable cyclic voltammogram of naval steel treated with a triangular potential perturbation. The potential sweep was 2.5 V s^{-1} and the anodic and cathodic switching potentials were 2.5 V and −2.5 V, respectively. The working electrolyte was 2 M aqueous sodium hydroxide and the perturbation was applied during 300 cycles. Stable cyclic voltammograms were run between −1.50 V and 1.50 V at 0.008 V s^{-1} in 0.50 M aqueous sodium nitrate containing dissolved oxygen. Temperature = 20 °C. The arrows indicate the potential cycling direction.

3.2.2. *Thermal treatment*

Figure 2(b) shows the stable cyclic voltammetric response of the steel surface after a thermal treatment (red-coloured). The current vs. potential profile is qualitatively similar to that of the polished naval steel, showing a hump and a single anodic peak but with lower intensities, i.e. the charge density involved under peak at 0.15 V was 70 μC cm^{-2}. An almost negligible reactivation peak can also be observed. Corrosion parameters in aerated 0.50 M sodium nitrate are $E_{corr} = -0.643$ V, $j_{corr} = 57.6$ μA cm^{-2}. These results show that the surface is more active to corrosion than the others.

3.2.3. *Triangular potential pre-treatment*

Figure 2(c) shows the cyclic voltammetric response of naval steels in aqueous 0.50 M sodium nitrate after 300 cycles of the triangular potential perturbation in a separate 2 or 5 M sodium hydroxide solution between −2.5 V and 2.5 V at 2.5 V s^{-1}. For this pre-treatment

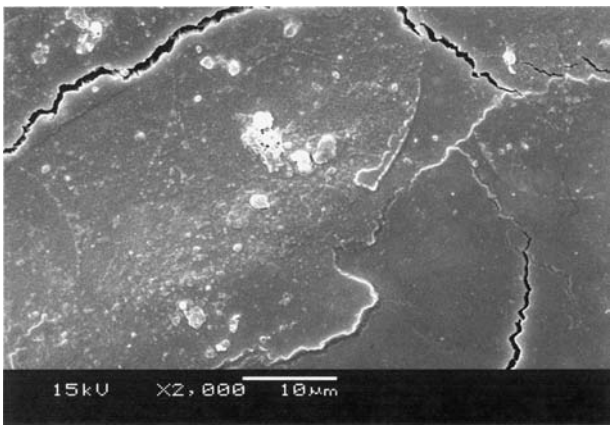

Fig. 3. SEM micrograph obtained after applying a chemical etching to naval steel surfaces. 10 μm. Magnification 2000×.

both concentrations of the alkaline solution produce the same electrochemical results. As a difference with respect to the polished surface, the onset potential for steel oxidation positively shifts to 0 V, and no reactivation occurs during the negative-going reverse scan. The anodic dissolution of the steel surface exhibits some linearity (ohmic contribution) and passivation is observed only in the reverse scan. In this case, the total anodic charge density corresponds to one monolayer, that is, 220 μC cm^{-2}. If the triangular perturbation pre-treatment is continued for more than 1000 cycles, the steel surface can no longer be stabilized in a cyclic voltammetric run and continuous dissolution without passivation is observed. Corrosion parameters after 300 cycles of the triangular potential perturbation in aerated 0.50 M sodium nitrate are $E_{corr} = -0.666$ V, $j_{corr} = 70$ μA cm^{-2}. In this case, it can be concluded that the electrochemical pre-treatment only promotes a more destabilized surface.

3.3. *The electrochemical behaviour of naval steels in alkaline solutions*

The behaviour of iron and non-stainless steels in aqueous sodium hydroxide has been reported elsewhere [25]. Figure 4 shows the repetitive voltammetric profile of a polished and chemical etched steel surface in 2 M sodium hydroxide run at a scan rate of 0.10 V s^{-1} between −1.5 and 0.6 V. One hump and five peaks have been found in the forward anodic scan and four peaks and a hump in the reverse cathodic scan. According to the literature [25, 26] hump I is related to a coupled process of the simultaneous bare iron dissolution and hydrogen electrosorption processes on a reduced iron surface [26]. Peaks II (15 μC cm^{-2}) and III (60 μC cm^{-2}) in the anodic sweep, while peaks VIII and IX (180 μC cm^{-2}) in the cathodic scan, are attributed to the $Fe(OH)_2$ formation and reduction to Fe in two steps [26]:

$$Fe + OH^- \leftrightarrow [Fe(OH)]_{ad} + e^- \qquad \text{(peaks II and IX)}$$

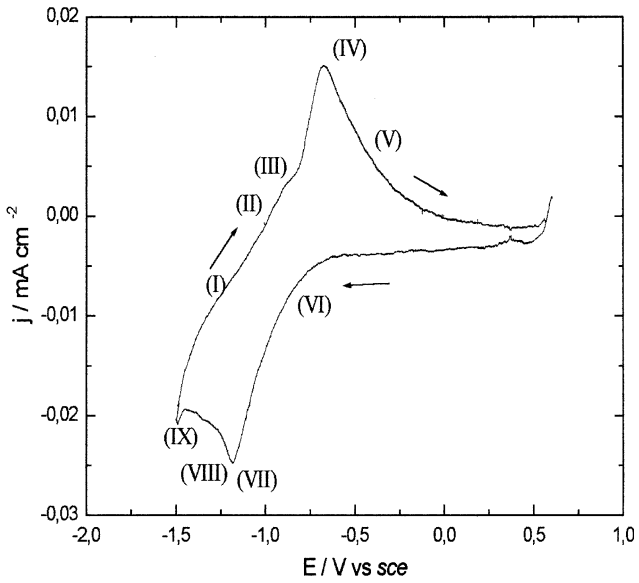

Fig. 4. Cyclic voltammogram of polished naval steel recorded from −1.50 to 0.60 V at 0.10 V s^{-1} in 2 M aqueous sodium hydroxide. Temperature = 20 °C. Peaks are labelled in Romans.

$$\left\{\begin{array}{l}[Fe(OH)]_{ad} + OH^- \leftrightarrow [FeO]_{ad} + H_2O + e^- \\ [FeO]_{ad} + OH^- \leftrightarrow HFeO_2^- \\ HFeO_2^- + H_2O \leftrightarrow \{Fe(OH)_2\} + OH^-\end{array}\right\} \quad \text{(peaks III and VIII)}$$

Peaks IV (620 μC cm^{-2}) and VII (350 μC cm^{-2}) are associated to the formation and reduction of magnetite from $Fe(OH)_2$, respectively [25]. From the ratio between both charge densities (Peak IV to peak VII charge ratio equal to 1.8) it can be concluded that not all the magnetite is reduced again to $Fe(OH)_2$ during the selected potential scan.

$$3\{Fe(OH)_2\} + 2OH^- \leftrightarrow \{Fe_3O_4\} + 4H_2O + 2e^- \quad \text{(peaks IV and VII)}$$

At potentials higher than −0.60 V, magnetite is partially oxidized to γ-FeOOH, peak V with 160 μC cm^{-2}, attributed [25] to

$$\{Fe_3O_4\} + H_2O + OH^- \leftrightarrow 3\{\gamma - FeOOH\} + e^- \quad \text{(peakV)}$$

In the course of the reactions and during cycling, γ-FeOOH chemically dehydrates to produce Fe_2O_3.

3.4. *Electrochemical surface modifications of naval steel surfaces by periodic potential programs*

It has been found that the application of a PPP can produce dramatic changes on the morphology and crystallography of metal electrodes [8, 10, 11]. In the case of ferrous metals, there are some papers dealing with the effects of periodic potential programs [15, 18]. None of these methodologies has been used in a controlled preferential growth of iron oxides. The development of iron oxides under a defined crystallography and roughness is faster in alkaline solutions than in acid solutions and can be better-controlled using periodic asymmetric potential perturbations [15, 16, 27]. Moreover, other authors [28] used other techniques such as laser pulsating lights under constant potential (or periodic potentials) on steel showing promising results in corrosion properties, i.e. the inhibition of the active dissolution was observed.

The first paper dealing with the application of periodic perturbations at metal electrodes is due to Cerviño et al. [29]. In this paper, it was found that (100) stepped crystallites developed after applying a frequency of 5 kHz to polycrystalline platinum between the anodic and cathodic solvent decomposition potentials. *SEM* micrographs of these surfaces exhibited large square and rectangular crystallites denoting the formation of facets with a [100] preferred crystallographic orientation. Moreover, it has been demonstrated that *ex situ STM* images [30] of these modified platinum surfaces are similar to those of true single crystals in the same electrolyte, except for a larger contribution of stepped domains.

The application of a square wave potential at non-noble electrodes with mean potential values larger than 1 V produces charge transfer involving solvent molecules with a preferential formation of certain bulk oxides. Previous results showed that it was possible to change the crystalline distribution of the metal by applying periodic perturbations [3]. In this work different conditions for the PPP techniques were applied from which two distinct groups were separated. In the first group, the results involving symmetric PPP with mean potential values lying before the onset of bulk iron oxides in 0.5 M sodium nitrate (ca. −0.7 V) were included. In the first process, the iron (and metal alloy) dissolution/reduction with hydroxide-containing species occurs. This means that it is possible to accumulate an excess of surface energy due to the fast iron hydroxide dissolution/reduction. The application of a PPP originates free energy excess and a redistribution of charges between iron and iron hydroxides (oxides) surface neighbours, resulting in new atomic and oxide arrangements.

In a second group, the results involving asymmetric PPP (and combined perturbations) were included, where the mean potential values cover the region of a net iron oxide formation. The application of an asymmetric PPP covering the stability region of the bulk iron oxides produces dramatic changes in the iron surface morphology. The process of iron oxide formation on iron is complicated, however there is agreement on the occurrence of reactions related to peaks II/IX at relatively large potentials. The kinetics of oxygen-containing species formation allows a further chemical oxidation of these adsorbates as explained above. This oxidation is largely activated by the presence of defects, which promotes the formation of kinks and steps.

These surface sites favour the formation of stepped planes [31].

We present now the main results on the application of symmetric, asymmetric and combined PPP to naval steel in strong alkaline solutions. The stability of the new oxide surfaces has been checked by open circuit potential decay in different media.

3.4.1. *The application of symmetric* PPP *on naval steels in alkaline solutions*

Figure 5(a) shows the repetitive cyclic voltammogram run at 0.10 V s^{-1} between −1.5 and 0.6 V in 2 M sodium hydroxide of a polished and chemical etched steel surface treated with a symmetric PPP. This perturbation is defined as follows; $f = 5$ kHz, $E_u = 2.0$ V and $E_l = -1.0$ V applied for 30 min in 2 M sodium hydroxide.

The electrochemical contour of the resulting surface is clearly different, since anodic and cathodic peaks are better defined. Moreover, peaks IV and VII (formation and dissolution of magnetite, respectively) are preferentially grown with respect to the other oxides or hydroxides. From the accumulated charges in the main peaks IV (1890 μC cm^{-2}) and VII (1460 μC cm^{-2}), it can be concluded that the reaction of ferrous hydroxide formation from magnetite (denoted by peak VII) is not complete, since the peak IV to peak VII charge ratio is ca. 1.3. Passivation is achieved at potentials much lower than expected, i.e. it starts at −0.15 V, that is, ca. 0.9 V less than the polished and chemical etched naval steel. Thus, passivation on steel is attained at much lower potentials than on a non-treated surface.

Similar symmetric PPP were applied varying the value of f, E_u and E_l in aqueous 2 M sodium hydroxide. The best results for corrosion parameters were found using a 5 kHz frequency in the ($E_u = 2.0$ V, $E_l = -1.0$ V) potential range. In this case, E_{corr} results −0.545 V and j_{corr} becomes 7 μA cm^{-2}, a value lower than that for the polished and chemical etched surface. After applying the symmetric PPP, *SEM* micrographs exhibit morphological changes characterized by globular oxide growths of high population densities (Figure 6(a)).

3.4.2. *The application of asymmetric* PPP *on naval steels in alkaline solutions*

Different asymmetric square wave potentials were used to grow a more densely packed protective oxide layer. The PPP with f_u ten times larger than f_i exhibited the best corrosion parameters in 0.50 M sodium nitrate, that is,

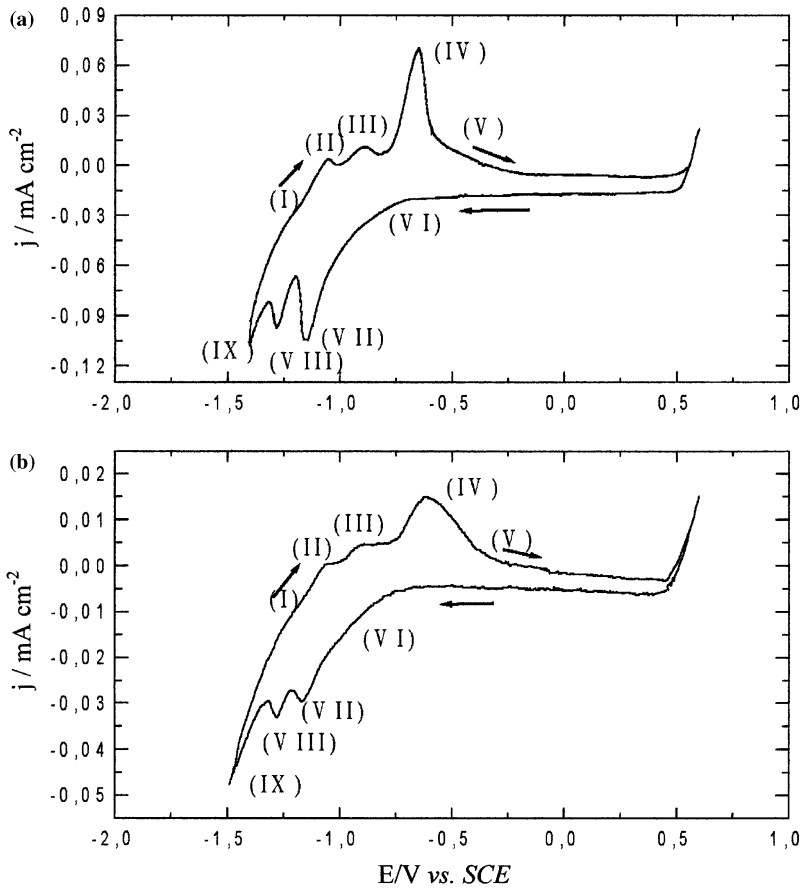

Fig. 5. Cyclic voltammogram of (a) naval steel treated with a symmetric square wave potential of $f = 5$ kHz, $E_u = 2.0$ V and $E_l = -1.0$ V during 30 min in aqueous 2 M sodium hydroxide; (b) naval steel subjected *to* a: (i) symmetric square wave of $f = 5$ kHz with $E_u = 2.0$ V and $E_l = -1.0$ V during 15 min in aqueous 2 M sodium hydroxide, and (ii) asymmetric square wave *of* $E_u = 2.0$ V $f_u = 18$ ms and $E_l = -1.0$ V $f_l = 2$ ms during 15 min in aqueous 2 M sodium hydroxide. All the voltammograms were recorded from −1.50 to 0.60 V at 0.10 V s^{-1} in 2 M aqueous sodium hydroxide. Temperature = 20 °C. Peaks are labelled in Romans.

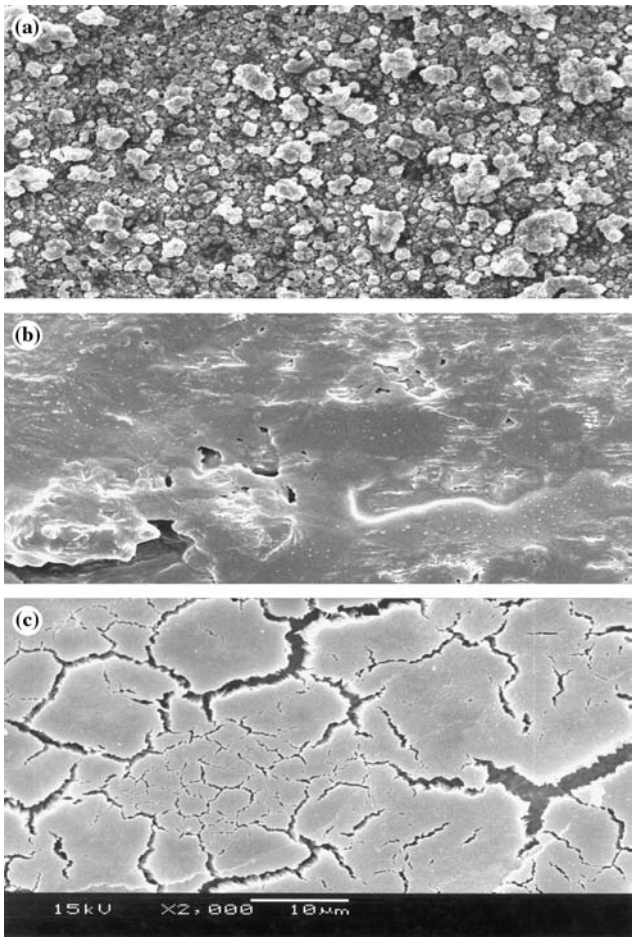

Fig. 6. SEM micrographs of naval steel surfaces obtained (a) after applying a symmetric potential perturbation of $f = 5$ kHz, $E_u = 2.0$ V and $E_l = -1.0$ V; (b) after applying an asymmetric potential perturbation *of* $E_u = 2.0$ V ($f_u = 18$ ms) and $E_l = -1.0$ V ($f_l = 2$ ms); (c) after applying a combined symmetric potential perturbation of $f = 5$ kHz, $E_u = 2.0$ V and $E_l = 1.0$ V; and an asymmetric potential perturbation *of* $E_u = 2.0$ V $f_u = 18$ ms) and $E_l = -1.0$ V ($f_l = 2$ ms). All the images are in 10 μm with a magnification 2000×.

lower j_{corr} values. Particularly in the case of $E_u = 2.0$ V ($f_u = 18$ ms) and $E_l = -1.0$ V ($f_i = 2$ ms), E_{corr} was −0.730 V. In this case, j_{corr} becomes 0.8 μA cm^{-2}, which is significantly lower than the value obtained for the polished and chemical etched steel surface. A comparison between the steel morphologies obtained from the asymmetric and symmetric PPP was conducted comparing *SEM* micrographs. It can be concluded that the oxide growth after the application of the asymmetric PPP produces a more densely packed oxide than with the symmetric signal, that is, an oxide characterized by a more compact and less rough surface (Figure 6(b)). The propagation of the oxide formation for the asymmetric PPP is typical of a nucleation and radial growth [32].

3.4.3. The application of a symmetric/asymmetric PPP *on naval steels in alkaline solutions*

Corrosion parameters were checked for different combined PPP by changing the sequence of the signals, frequency and potential limits.

The repetitive voltammetric profile of naval steels subjected to one of the combined PPP in alkaline solutions is presented in Figure 5(b), consisting of a first symmetric squarewave of $f = 5$ kHz with $E_u = 2.0$ V and $E_l = -1.0$ V during 15 min in 2 M sodium hydroxide,and a second asymmetric signal of $E_u = 2.0$ V, $f_u = 18$ ms and $E_l = -1.0$ V, $f_i = 2$ ms in the same conditions. The electrochemical features in alkaline solutions are similar to those presented in Figure 5(a). However, the intensities of peaks IV and VII are lower than those obtained after the application of a single symmetric PPP. Nevertheless, while the charge density under peak IV is exactly the same (1890 μC cm^{-2}), the charge density under peak VII (1030 μC cm^{-2}) is less for the application of the asymmetric than the symmetric PPP mode. This is probably due to the formation of an intermediate soluble species such as, $HFeO_2^-$ [7, 25]. The consequence of this fact is that it is not possible to grow a permanent protective magnetite-film because of the existence of soluble species, i.e. the peak IV to peak VII charge ratio is equal to 1.8. In some cases the cyclic voltammograms show oscillations in the anodic region, a fact related to the appearance of cracks – without preferential propagation direction – found in the *SEM* micrographs (Figure 6(c)).

The corrosion parameters ranged as follows $-0.28\ V \le E_{corr} \le -0.08$ V with a 3.2 nA cm$^{-2} \le j_{corr} \le$ 0.25 μA cm^{-2}. The lower limit is significantly smaller than those found after using the other potential perturbations.

3.5. *The stability of the oxide surfaces grown by* PPP *in different electrolytes*

Figure 7(I) shows the superimposed decays of the open-circuit potentials for naval electrodes in 0.50 M sodium nitrate. It can be seen that the best performance is achieved for the symmetric PPP technique where the surface oxide stays stable up to 780 s.

In the case of nitrate and chloride containing solutions 7(II) and 7(III), the situation is different because of the nature of the anions in the electrolytes. For example, for solution containing 0.50 sodium nitrate and 0.60 M sodium chloride 7(II), the long term exposure of the oxide obtained from the combined PPP technique is the best, i.e. −0.524 V compared with −0.644 V of the non-treated sample. However, in the case of the oxides obtained from the symmetric PPP technique the early stages of the open-circuit potential curve have better performance than those obtained from the combined one. The difference between the open circuit potential decays of the PPP treated samples and non-treated samples after 1 h is ca. 0.15 V showing the long-term effects of the periodic potential techniques. In the case of a potential decay in 0.60 M sodium chloride 7(III) the best performance is again achieved for the combined PPP technique where the surface oxide stays stable up to 340 s. Moreover, the corresponding long-time value of the open-circuit

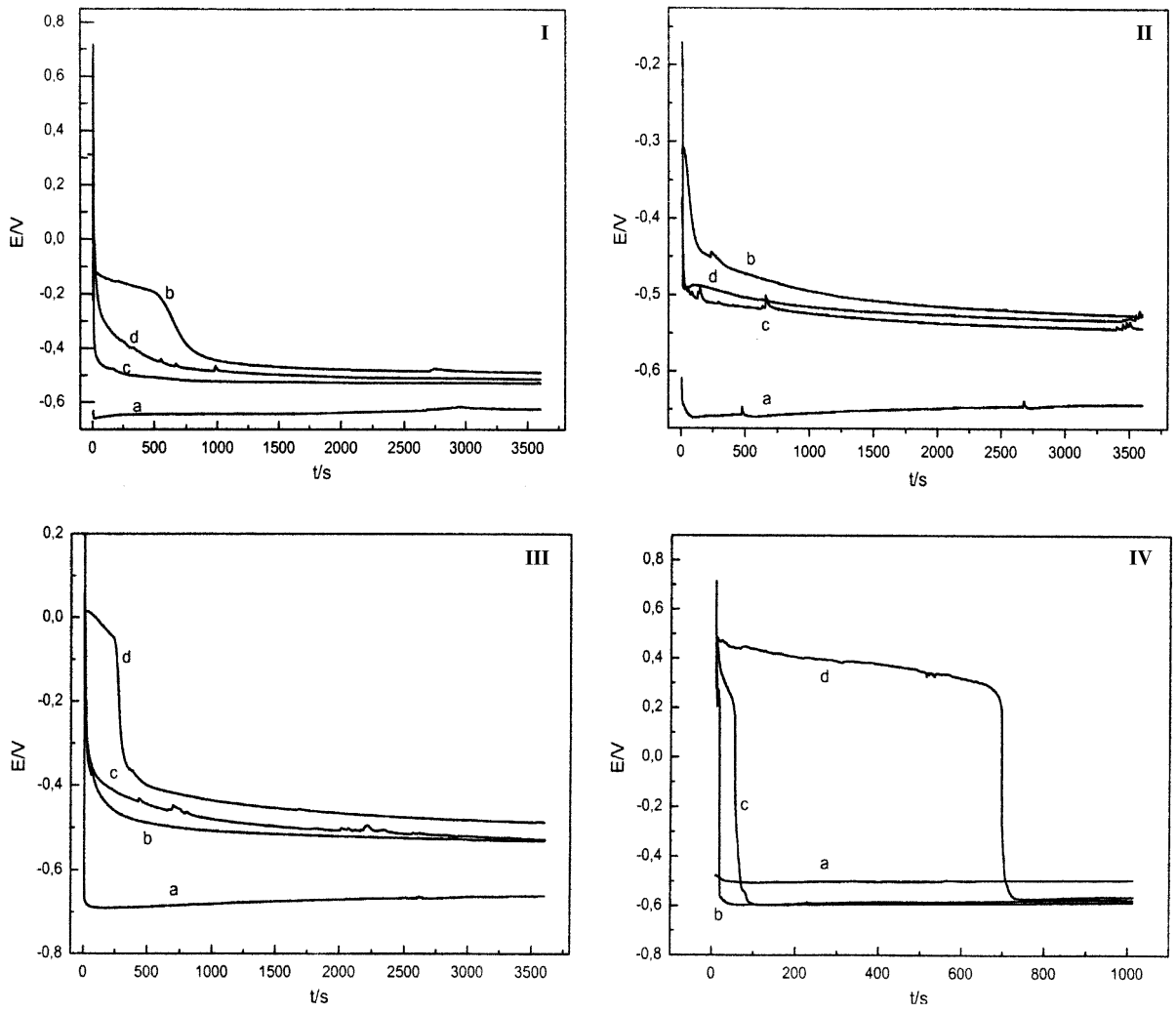

Fig. 7. Open circuit potential time decays for naval steel electrodes (a) treated by symmetric (b), asymmetric (c) and combined PPP (d) in: (I) 0.50 M sodium nitrate, (II) 0.60 M sodium chloride and 0.50 M sodium nitrate, (III) 0.60 M sodium chloride and (IV) 0.10 M sulphuric acid solution.

potential is −0.488 V compared with the 0.678 V of the non-treated naval steel surface.

Figure 7(IV) shows the superimposed decays of the open-circuit potentials for naval steel electrodes in 0.10 M sulphuric acid. It can be seen that the surface oxide form by the application of a combined PPP technique is stable up to 710 s, whereas the fastest potential decays correspond when using the asymmetric (95 s) and symmetric signals (20 s). The performance of the combined treatment is clearly seen through the initial positive free potential of about 0.5 V. In all cases, the potential decay is simple with clearly defined transition times.

3.6. *The influence of chloride and nitrate to naval steel corrosion for long-time exposures*

The influence of the exposure time after the application of the PPP techniques has been checked using potentiostatic polarization curves of naval steels in 0.01, 0.10 and 0.60 M of sodium chloride in 0.50 M sodium nitrate after 1 h, 24 h, 48 h and 1 week. The electrodes have been treated according to the symmetric, asymmetric and combined symmetric–asymmetric PPP techniques explained above. Table 2 shows the values obtained for E_{corr} in the different electrolytes. Independent of the electrolyte composition, stable values of E_{corr} are obtained after 1 h of exposure time.

For the non-treated samples, it can be concluded that E_{corr} becomes more negative when the chloride concentration is increased, as expected for a chloride induced corrosion process on steel. However, for larger exposure times an increase in the E_{corr} values is observed. In the case of a 0.50 M sodium nitrate solution, the increase in the values of E_{corr} is due to the passivation process induced by nitrate anions [21].

On the other hand, the application of a symmetric PPP technique for low chloride concentrations shows promising results, i.e. the values of E_{corr} after 1 h are almost 0.1 V higher than those for the non-treated samples. The disappearance of the surface oxides after this time of exposures produces a fast decrease in the E_{corr} values for 0.60 M sodium chloride solutions. In the rest of the samples the competition between chloride

Table 2. Time dependent E_{corr} (V ± 0.005 V) values for non-treated naval steel and samples treated with symmetric, asymmetric and combined *PPP* techniques in 0.50 M sodium nitrate, 0.60 M sodium chloride and 0.50 M sodium nitrate + 0.01, 0.10 or 0.60 M sodium chloride

Electrolyte	1 hour	24 hours	48 hours	1 week
Non – treated samples				
0.50 M $NaNO_3$	−0.627	−0.619	−0.639	−0.599
0.50 M $NaNO_3$ + 0.01 M NaCl	−0.635	−0.607	−0.572	−0.582
0.50 M $NaNO_3$ + 0.10 M NaCl	−0.642	−0.585	−0.600	−0.638
0.50 M $NaNO_3$ + 0.60 M NaCl	−0.656	−0.626	−0.603	−0.636
0.60 M NaCl	−0.696	−0.662	−0.660	−0.658
Symmetric PPP treated samples				
0.50 M $NaNO_3$	−0.545	−0.631	−0.632	−0.627
0.50 M $NaNO_3$ + 0.01 M NaCI	−0.585	−0.653	−0.636	−0.593
0.50 M $NaNO_3$ + 0.10 M NaCI	−0.565	−0.663	−0.619	−0.636
0.50 M $NaNO_3$ + 0.60 M NaCI	−0.664	−0.639	−0.590	−0.637
0.60 M NaCI	−0.676	−0.719	−0.720	−0.732
Asymmetric PPP treated samples				
0.50 M $NaNO_3$	−0.597	−0.618	−0.602	−0.597
0.50 M $NaNO_3$ + 0.01 M NaCl	−0.616	−0.607	−0.590	−0.580
0.50 M $NaNO_3$ + 0.10 M NaCl	−0.599	−0.594	−0.590	−0.582
0.50 M $NaNO_3$ + 0.60 M NaCl	−0.624	−0.583	−0.594	−0.613
0.60 M NaCl	−0.682	−0.647	−0.666	−0.677
Combined PPP treated samples				
0.50 M $NaNO_3$	−0.527	−0.614	−0.616	−0.619
0.50 M $NaNO_3$ + 0.01 M NaCl	−0.557	−0.570	−0.551	−0.533
0.50 M $NaNO_3$ + 0.10 M NaCl	−0.588	−0.579	−0.578	−0.578
0.50 M $NaNO_3$ + 0.60 M NaCl	−0.621	−0.619	−0.601	−0.595
0.60 M NaCl	−0.657	−0.683	−0.672	−0.650

and nitrate is observed in the E_{corr} oscillations. In the case of asymmetric and combined PPP techniques, the behaviour is different since the sample resists more effectively to higher concentrations of chloride than symmetric perturbations. After one week there is no difference between the values of E_{corr} obtained with asymmetric and combined PPP techniques with respect to the non-treated sample. The effect of chloride in solution is more important for treated samples, because the morphology of the surface is changed during both the stabilisation of the new oxide and the corrosion process itself.

4. Conclusions

The characterization of naval steel oxides produced by periodic potentials (such as the PPP) by cyclic voltammetric profiles, open-circuit potential decays and scanning microscopy shows that a more protective layer can be obtained by applying square wave potentials. Among these processes, oxide layers obtained after a combined (symmetric and asymmetric) potential routine results in more negative corrosion potentials, especially in the case of high chloride concentrations (0.60 M). The influence of chloride (aggressive anion) on naval steel surfaces in the presence of nitrate (passivating anion) solutions is a competitive process, which also depends on the presence of surface oxides. For low chloride concentrations (less than 0.10 M), steel surfaces treated with a symmetric signal gives rise to surface layers exhibiting good performances at exposure times lower than 1 week. On the other hand, the application of an asymmetric or a combined potential routine to naval steel gives rise to better results in the case of chloride concentrations larger than 0.10 M. However, corrosion currents in the case of steel surfaces subjected to a combined potential routine are lower than expected, i.e. lower than 0.25 μA cm^{-2} in an oxygenated 0.50 M nitrate solution. Best results for corrosion resistance were obtained in the case of the combined potential perturbation after chemical etching. This perturbation consists of a symmetric square wave of $f = 5$ kHz with $E_u = 2.0$ V and $E_t = -1.0$ V for 15 min followed by an asymmetric signal of $E_u = 2.0$ V, $f_u = 18$ ms and $E_t = -1.0$ V, $f_i = 2$ ms for the same time. The morphology of the new surface according to *SEM* shows a significant population of cracks, suggesting the necessity of a final thermal or high current density treatment.

Acknowledgements

PEDECIBA (United Nations), Universidad de la República and Marine Force Group support this work. CFZ is a researcher at PEDECIBA Chemistry.

References

1. N.A. North, *Int. J. Underwater Arch. Underwater Explr.* **5** (1976) 253.
2. I.D. Mc Leod, Trends in Corr. Research (pub. Council Scientific Research, India, 1993), p. 221.

3. C.F. Zinola, ''New corrosion methodologies for naval steel protection'' CSIC Project (1999–2001). Universidad de la República, Montevideo, Uruguay.
4. 'An in situ study of the corroded hull of HMVS Cerberus', I. Mc.Leod, 13th. Meeting of the International Corrosion Council, (1994), p. 125.
5. Y. González, M.C. Lafont and N. Pebere, *J. Appl. Electrochem.* **26** (1996) 1259.
6. T.P. Hoar, *Inst. of Corr. Tech.* **32** (1972) 19.
7. C. Andrade, M. Keddam, X.R. Novoa, M.C. Pérez, C.M. Rangel and H. Takenouti, *Electrochim. Acta* **46** (2001) 3905.
8. M.E. Martins, C.F. Zinola, G. Andreasen, R.C. Salvarezza and A.J. Arvia, *J. Electroanal. Chem.* **445** (1998) 135.
9. A. Czerwinski and J. Sobkowski, *J. Electroanal. Chem.* **55** (1974) 391.
10. A. Visintín, J.C. Canullo, W.E. Triaca and A.J. Arvia, *J. Electroanal. Chem.* **239** (1988) 67.
11. W.E. Triaca, T. Kessler, J.C. Canullo and A.J. Arvia, *J. Electrochem. Soc.* **134** (1987) 1165.
12. C.F. Zinola, A. Castro Luna, W.E. Triaca and A.J. Arvia, *J. Appl. Electrochem.* **24** (1994) 119.
13. S.A. Bilmes, M.C. Giordano and A.J. Arvia, *Can. J. Chem.* **66** (1988) 2259.
14. C.F. Zinola and A. M. CastroA. Luna, *Corros. Sci.* **37** (1995) 1919.
15. S.B. Lalvani and G. Zhang, Corros. Sci. **37** (1995) 1567, 1583.
16. S.B. Lalvani, J.C. Kang and N. Mandich, *Corros. Sci.* **40** (1998) 201.
17. S.B. Lalvani, J.C. Kang and M. Murthy, *Corros. Sci.* **37** (1995) 1599.
18. F. Mansfeld, S.H. Lin and L. Kwiatkowski, *Corros. Sci.* **34** (1993) 2045.
19. A.E. Bolzán, A.M. Castro Luna, A. Visintín, R.C. Salvarezza and A.J. Arvia, *Electrochim. Acta.* **33** (1998) 1743.
20. G. Rocchini, *Corros. Sci.* **41** (1999) 2353.
21. D. Sazou and M. Pagitsas, *Electrochim. Acta.* **47** (2002) 1567.
22. A. Saraby-Reintejes, *Electrochim. Acta.* **30** (1985) 403.
23. H. Prinz and H.H. Strehblow, *Corros. Sci.* **40** (1998) 1671.
24. J.S. Noh, N.J. Laycock, W. Gao and D.B. Wells, *Corros. Sci.* **42** (2000) 2069.
25. A. Wieckowski and E. Ghali, *Electrochim. Acta.* **30** (1985) 1423.
26. B. Kabanov, R. Burshtein and A.K.N. Frumkin, *Discuss. Faraday Soc.* **1** (1947) 259.
27. Y. Zuo, H. Wang, J. Zhao and J. Xiong, *Corros. Sci.* **44** (2002) 13.
28. C. Carboni, P. Peyre, G. Béranger, C. Lemaitre and R. Fabbro, 'Improvement of the pitting corrosion resistance of AISI 316L stainless steel by laser shock waves', 52nd San Francisco ISE Meeting. Corrosion, Electrodeposition and Surface Treatment Section, Abstract CI-53, 2–7 September 2001.
29. M. Cerviño, W.E. Triaca and A.J. Arvia, *J. Electroanal. Chem.* **182** (1985) 51.
30. J. Gómez, L. Vásquez, A.M. Baró, N. García, C.L. Perdriel, W.E. Triaca and A.J. Arvia, *Nature* **323** (1986) 612.
31. R.R. Adzic, 'Modern Aspects of Electrochemistry', N. 18, Chap. 5, p. 163, R.E. White, B.E. Conway, E.B. Yeager (Eds) Plenum Press, New York (1988).
32. G.A. Somorjai, 'Introduction to Surface Chemistry and Catalysis', Chap. 2, J. Wiley & Sons (ed.) New York (1994).